Enhanced Stability of Cu−BTC MOF via Perfluorohexane Plasma-Enhanced Chemical Vapor Deposition

ARTICLE *in* JOURNAL OF THE AMERICAN CHEMICAL SOCIETY · JANUARY 2012

Impact Factor: 12.11 · DOI: 10.1021/ja211182m · Source: PubMed

5 AUTHORS, INCLUDING:

Jared B DeCoste
United States Army
29 PUBLICATIONS **357** CITATIONS
SEE PROFILE

Gregory W. Peterson
United States Army
77 PUBLICATIONS **838** CITATIONS
SEE PROFILE

Martin Smith
Defence Science and Technology Laboratory …
10 PUBLICATIONS **178** CITATIONS
SEE PROFILE

Colin Willis
Defence Science and Technology Laboratory …
22 PUBLICATIONS **412** CITATIONS
SEE PROFILE

JACS
JOURNAL OF THE AMERICAN CHEMICAL SOCIETY
Communication
pubs.acs.org/JACS

Enhanced Stability of Cu-BTC MOF via Perfluorohexane Plasma-Enhanced Chemical Vapor Deposition

Jared B. Decoste,*[,†] Gregory W. Peterson,[†] Martin W. Smith,[‡] Corinne A. Stone,[‡] and Colin R. Willis[‡]

[†]Edgewood Chemical Biological Center, 5183 Blackhawk Road, Aberdeen Proving Ground, Maryland 21010, United States
[‡]Defence Science and Technology Laboratory, Porton Down, Salisbury, Wiltshire SP4 0JQ, United Kingdom

Supporting Information

ABSTRACT: Metal organic frameworks (MOFs) are a leading class of porous materials for a wide variety of applications, but many of them have been shown to be unstable toward water. Cu-BTC (1,3,5 benzenetricarboxylic acid, BTC) was treated with a plasma-enhanced chemical vapor deposition (PECVD) of perfluorohexane creating a hydrophobic form of Cu-BTC. It was found that the treated Cu-BTC could withstand high humidity and even submersion in water much better than unperturbed Cu-BTC. Through Monte Carlo simulations it was found that perfluorohexane sites itself in such a way within Cu-BTC as to prevent the formation of water clusters, hence preventing the decomposition of Cu-BTC by water. This PECVD of perfluorohexane could be exploited to widen the scope of practical applications of Cu-BTC and other MOFs.

Metal organic frameworks (MOFs) have become a leading class of porous materials for applications, such as gas storage,[1] separations,[2] catalysis,[3] and even toxic gas removal.[4−6] These materials show unprecedented ability to tailor functionality for targeted chemical interaction. In toxic gas removal, several studies have shown that MOFs are able to provide substantial protection as compared to other sorbents.[5] Yet, one of the major shortcomings of several classes of MOFs is their instability in the presence of moisture.[7−11]

$Cu_3(BTC)_2$, (1,3,5 benzenetricarboxylic acid, BTC) or HKUST-1 (herein referred to as Cu-BTC), has previously been investigated for numerous applications, including ammonia removal.[12] The material was found to have an exceptionally high ammonia loading, but at the expense of framework stability. Due to a combination of ammonia and moisture, the structure essentially was shown to completely disintegrate. Further studies on Cu-BTC by Gul-E-Noor et al. using ^{1}H and ^{13}C solid-state NMR indicated that moisture itself is capable of degrading the MOF structure, rendering it ineffective for use in a multitude of applications.[11]

Generally speaking, many MOFs that are highly active toward toxic chemicals, and/or separations are prone to decomposition due to moisture. Finding a means of stabilizing these structures would allow for their use in ambient applications where moisture is omnipresent. Montoro and co-workers recently investigated a hydrophobic analog of MOF-5 (IRMOF-1) for use in capturing nerve and mustard simulants.[4] Yang et al. modified MOF-5 by placing methyl groups on the linking units, which exhibited unchanged X-ray diffraction (XRD) patterns after days of exposure to ambient humidity.[13] Yet, these methods may change the inherent nature and chemistry of the MOF, and these methods are not possible for a full range of MOFs.

Yoo and co-workers recently addressed this issue using a surfactant-assisted drying technique and found IRMOF-3 to be stable to ambient moisture after one month.[14] In this communication, we investigate an alternative method for postsynthetically modifying Cu-BTC by a plasma-enhanced chemical vapor deposition (PECVD) of perfluorohexane (PFH), referred to throughout this manuscript as Cu-BTC Plasma.

Cu-BTC was purchased from Sigma-Aldrich as Basolite C 300 in powder form. Cu-BTC plasma was produced using a PECVD method[15,16] with a perfluorohexane precursor in a plasma reactor and is discussed in depth in the Supporting Information.

After treatment, Cu-BTC plasma was characterized to determine any structural changes. Powder XRD (PXRD) patterns (Figure S3, Supporting Information) indicate the structure of Cu-BTC plasma is analogous to Cu-BTC, and both match the simulated pattern. There is a decrease in intensity of peaks that are indicative of long-range order. This is evidence of pore filling by PFH or nonperiodic minor structural changes. Upon immersion in water at room temperature, the PXRD pattern of Cu-BTC completely changed over the period of 24 h (Figure 1a), signifying major structural changes taking place. However, the PXRD pattern of Cu-BTC plasma (Figure 1b) was virtually unchanged over the same period. The PXRD pattern of Cu-BTC after 4 h of immersion in water shows characteristics of both the unperturbed Cu-BTC and the 24 h immersed Cu-BTC. The gradual decomposition of Cu-BTC has been shown to accelerate with increasing molar equivalents of water as described in depth by Gul-E-Noor.[11] The water stability of Cu-BTC plasma may extend its useful applications beyond humidity sensing[17] and into the realm of desiccants as its crystal structure is not affected by high-humidity levels.[18]

The ^{19}F magic angle spinning (MAS) nuclear magnetic resonance (NMR) spectra of Cu-BTC, Cu-BTC plasma, and neat PFH can be seen in Figure 2. There are no ^{19}F chemical shifts in the Cu-BTC spectrum, which is consistent with the absence of fluorinated material being introduced to Cu-BTC. The Cu-BTC plasma sample shows a major presence of

Received: November 29, 2011
Published: January 9, 2012

   dx.doi.org/10.1021/ja211182m | J. Am. Chem.Soc. 2012, 134, 1486−1489

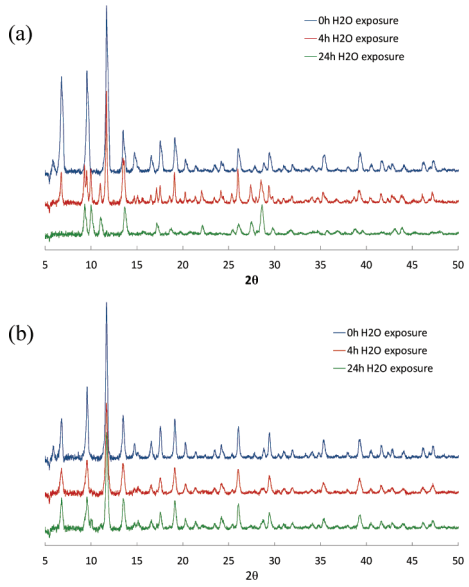

Figure 1. PXRD patterns for (a) Cu-BTC and (b) Cu-BTC plasma after immersion in water at room temperature for 0, 4, and 24 h.

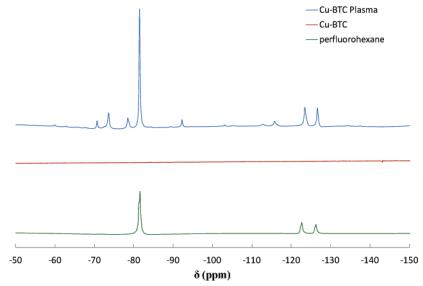

Figure 2. ^{19}F MAS NMR of Cu-BTC plasma, Cu-BTC, and neat PFH. All spectra are referenced to an external hexafluorobenzene reference $\delta \approx -165$ ppm.

perfluorohexane with chemical shifts at $\delta \approx -81$, -123, and -127 ppm. The chemical shifts at $\delta \approx -74$ and -78 ppm correspond to other CF_3 species that are present in the material.[19] All other chemical shifts in the ^{19}F MAS NMR spectrum of Cu-BTC plasma correspond to spinning sidebands approximately 6 kHz (the spinning speed of the rotor) away from the corresponding parent signal. The spinning sidebands stem from PFH being in a much more restricted environment when in the Cu-BTC plasma than in the neat sample.[20] The presence of perfluorohexane and a minor presence of other perfluoro products without evidence of polymerization in Cu-BTC plasma is consistent with the exposure of perfluorohexane to plasma by Shard et al.[21]

Due to its microporous nature, it is unlikely that plasma ignition of PFH occurs within the pores of Cu-BTC. The pores of Cu-BTC have a diameter ≈0.9 nm, while the characteristic plasma debye length is 2 μm < λ_D < 7 mm. This supports the hypothesis that the CF_3 species that are seen in the ^{19}F MAS NMR are from the diffusion of reactive CF_3 species across the plasma−solid interface.[22] Chemical reaction with the internal surface of the pores occurs as CF_3 diffuses. As the internal pores are populated with nonperiodic CF_3 groups, the diffusion of PFH becomes more favorable. The presence of CF_3 groups on the surface of the pores also adds to the hydrophobicity of the material, which actually causes the material to float in liquid water. When ^{19}F MAS NMR was performed on samples of Cu-BTC directly exposed to liquid or gaseous PFH followed by light heating, no presence of fluorinated material could be detected, meaning the population of the internal pore surface with CF_3 groups plays an integral role in PFH loading.

Nitrogen isotherms of Cu-BTC and Cu-BTC plasma (Figure S4, Supporting Information) show a decrease in BET surface area from 1468 to 1088 m^2/g (25.9%) and in total pore volume from 1.01 to 0.69 cc/g (31.7%). The BET surface area of Cu-BTC is consistent with data published elsewhere.[23,24] The decrease in surface area is larger than the weight percent of PFH loaded (determined by TGA), which is consistent with PFH blocking nitrogen adsorption sites and/or micropore accessibility. The size and ability of PFH to rotate about its C−C bonds give it the ability to extend across the window openings, acting as a strut and effectively block corner sites, making them inaccessible to nitrogen.

Scanning Electron Microscopy (SEM) images (600X magnification) of Cu-BTC and Cu-BTC plasma before and after exposure to 90% relative humidity at 25 °C are shown in Figure 3 (full images can be seen Figure S5, Supporting Information). Cu-BTC crystals with smooth surfaces, containing few irregularities and no cracking can be seen for both Cu-BTC (Figure 3a) and Cu-BTC plasma (Figure 3c) before exposure to water. The SEM images after exposure to water for Cu-BTC (Figure 3b) and Cu-BTC plasma (Figure 3d) show a difference in how the crystal structure reacts to humidity. The untreated Cu-BTC shows cracking of its surfaces and very little regularity in its structure. However, the crystal structure of Cu-BTC plasma was able to withstand the presence of high levels of humidity while maintaining its smooth surfaces and without noticeable surface cracking.

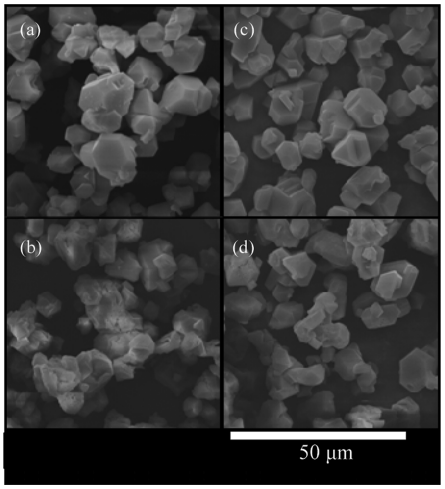

Figure 3. SEM images of (a) Cu-BTC, (b) Cu-BTC after exposure to 90% humidity, (c) Cu-BTC plasma, and (d) Cu-BTC plasma after exposure to 90% humidity.

Thermogravimetric analysis (TGA) was used to determine that the desorption of PFH from Cu-BTC occurs at 175 °C (Figure S6, Supporting Information). Integration of the first derivative peaks from the TGA data shows that PFH constitutes 16.1 wt % of the Cu-BTC plasma material when vacated of all water. The data also shows two distinct water desorption temperatures, 65 and 115 °C. According to Castillo et al.[25] the first siting of water occurs at site I, as seen in Figure 4, when using the convention set forth by Liu et al.[24] Site I corresponds to water molecules that are coordinated with Cu

dx.doi.org/10.1021/ja211182m | J. Am. Chem.Soc. 2012, 134, 1486−1489

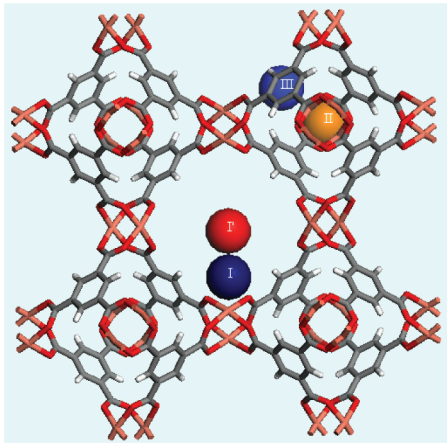

Figure 4. Representation of sorption sites I, I′, II, and III in Cu-BTC viewed along the [100] direction.

atoms. The second siting of water occurs at sites I′ (the large cage interior), this siting occurs through hydrogen bonding with water molecules adsorbed at site I. Water molecules are not found at sites II or III by Castillo et al., supporting our TGA results that only two distinct water desorption events occur. Site I, which has direct interaction with the Cu atoms, has a free energy of adsorption of −29.1 kJ/mol, compared to −8.1 kJ/mol for site I′. Therefore site I corresponds to water molecules desorbing at higher temperatures than site I′.[25]

Cu-BTC plasma shows a significant decrease in site I′ water desorption. This is further evidence of the siting of the hydrophobic PFH at site I′ or near enough as to affect water molecules in this region. Through simulation studies, it has been seen that nonpolar and quadrapolar molecules typically site themselves away from the Cu atoms.[26−30] Small nonpolar and quadrapolar molecules, such as methane and carbon dioxide, are preferentially adsorbed at the interior of the octahedral cage at site II, followed by sites III and I′.

Grand canonical Monte Carlo (GCMC) simulations of adsorption of 32 PFH molecules, corresponding to the loading levels determined from TGA, were performed on a 2 × 2 × 2 unit cell of Cu-BTC. Details of the calculations can be found in the Supporting Information.[26,31,32] PFH calculations were based on those used by Watkins and Jorgensen.[33] It is observed that site I′ is the preferential site for PFH siting, as can be seen in Figure 5. The bulky nature of PFH makes sites II and III relatively inaccessible leaving site I′ as the only site for PFH adsorption. It can be clearly seen in the [110] view that PFH does not site on the axis of the Cu−Cu bonds (Site I). The siting of PFH away from site I allows for water molecules to still coordinate with Cu atoms in Cu-BTC, but the hydrophobic nature of PFH in the pores would prevent the formation of water clusters at higher humidity levels as suggested for water siting in MOFs by Küsgens et al.[18] The prevention of water molecules from forming clusters at site I′ by PFH in Cu-BTC plasma also supports the decrease in site I′ water desorption in the TGA data.

Peterson et al. have shown the ability of Cu-BTC to adsorb large amounts of ammonia.[12] The addition of PFH plasma did not diminish the overall capacity of Cu-BTC for ammonia, as may be expected by pore filling, but it in fact enhanced its ammonia capacity (breakthrough curves in Figures S7 and S8, Supporting Information). The capacity of Cu-BTC and Cu-BTC plasma at conditions of 0% and 80% RH can be seen in Table 1. Petit et al. have shown through experimental and theoretical methods that ammonia is strongly attracted to the Cu−Cu dimers in Cu-BTC, which can account for approximately 5 mmol/g of ammonia adsorption.[34] The remainder of ammonia capacity by Cu-BTC can be attributed to other sites and intermolecular hydrogen bonding. The breakthrough curves at 80% RH show that even though the initial breakthrough of Cu-BTC plasma occurs earlier, likely due to the reduced porosity and surface area compared to Cu-BTC, there is actually an overall increase in ammonia capacity. The step-like shape of the breakthrough curve is indicative of a combination of mass transfer limitations (from the co-adsorbed PFH) and the migration of ammonia to reactive metal sites. This enhancement in ammonia capacity by Cu-BTC plasma can best be explained by the increased stability of Cu-BTC at both RH conditions. The resulting stability slows and/or eliminated the collapse of the pore structure and increases the ability to maintain more of its crystallinity in the presence of

Table 1. NH_3 Capacities of Cu-BTC and Cu-BTC Plasma

conditions	Cu-BTC (mol/kg)	Cu-BTC plasma (mol/kg)
0% RH	6.4	8.7
80% RH	10.4	11.8

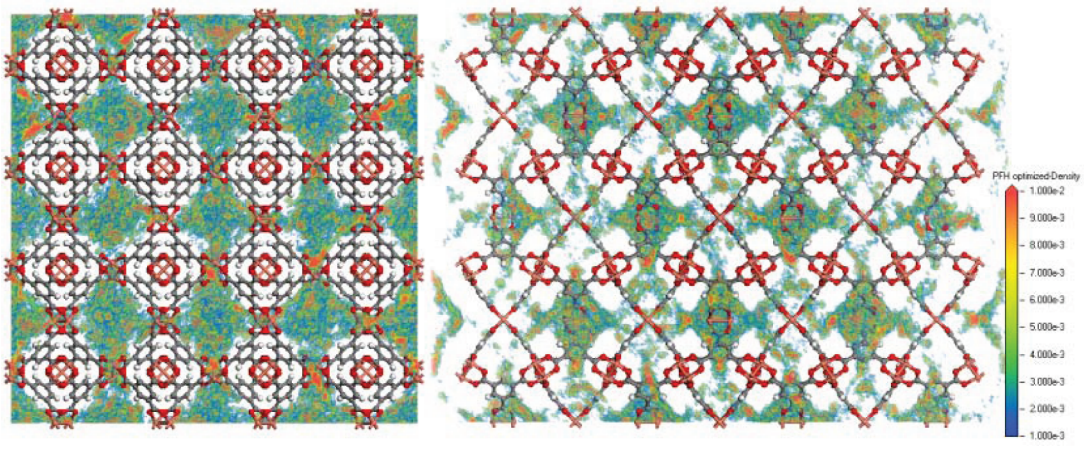

Figure 5. GCMC simulations of the adsorption of PFH in Cu-BTC viewed along the [100] (left) and [110] (right) directions.

dx.doi.org/10.1021/ja211182m | J. Am. Chem.Soc. 2012, 134, 1486−1489

ammonia and/or water. The behavior is illustrated in Figure S9, Supporting Information.

The enhancement of stability of Cu-BTC plasma seems to be from the ability of PFH to prevent the formation of water and/or ammonia clusters around the Cu sites as well as the ability of PFH to act as a strut to prevent the collapsing of pores. It was suggested by Peterson et al. that 4 equiv of water (or ammonia) for every Cu−Cu dimer are necessary for the breakdown of Cu-BTC to $Cu(OH)_2$.[12] With hydrophobic PFH sited in the large pores, the formation of clusters large enough to break apart Cu-BTC would be significantly hindered even when subjected to high humidity values or submersion in H_2O.

In summary, we have reported that treatment with plasma PFH enhances the stability of Cu-BTC against degradation by water. The overall crystal structure of Cu-BTC is maintained when submerged in water, and an enhancement of ammonia adsorption capacities gives Cu-BTC plasma broad appeal for many potential applications. Future work plans include extending this work to other MOFs including the highly water unstable IRMOF series (MOF-5 analogs), PECVD of other perfluoroalkanes on Cu-BTC, and testing the long-term effects of water on PECVD treated Cu-BTC for use in practical applications.

■ ASSOCIATED CONTENT

Ⓢ Supporting Information

Experimental procedures, PXRD patterns, nitrogen isotherms, SEM images, TGA data, and ammonia breakthrough curves. This material is available free of charge via the Internet at http://pubs.acs.org.

■ AUTHOR INFORMATION

Corresponding Author

jared.b.decoste2.ctr@mail.mil

■ ACKNOWLEDGMENTS

This research was performed while J.B. DeCoste held a National Research Council Research Associateship Award at the Edgewood Chemical Biological Center. The authors thank the Defense Threat Reduction Agency for funding under project number BA07PRO104, Bryan Schindler for his assistance in molecular modeling, and Matthew Browe for breakthrough testing.

■ REFERENCES

(1) Xiao, B.; Wheatley, P. S.; Zhao, X.; Fletcher, A. J.; Fox, S.; Rossi, A. G.; Megson, I. L.; Bordiga, S.; Regli, L.; Thomas, K. M.; Morris, R. E. *J. Am. Chem. Soc.* **2007**, *129*, 1203.
(2) Yaghi, O. M.; Li, G. M.; Li, H. L. *Nature* **1995**, *378*, 703.
(3) Mueller, U.; Schubert, M.; Teich, F.; Puetter, H.; Schierle-Arndt, K.; Pastre, J. *J. Mater. Chem.* **2006**, *16*, 626.
(4) Montoro, C.; Linares, F.; Quartapelle Procopio, E.; Senkovska, I.; Kaskel, S.; Galli, S.; Masciocchi, N.; Barea, E.; Navarro, J. A. R. *J. Am. Chem. Soc.* **2011**, *133*, 11888.
(5) Glover, T. G.; Peterson, G. W.; Schindler, B. J.; Britt, D.; Yaghi, O. *Chem. Eng. Sci.* **2011**, *66*, 163.
(6) Britt, D.; Tranchemontagne, D.; Yaghi, O. M. *Proc. Natl. Acad. Sci. U.S.A.* **2008**, *105*, 11623.
(7) Schroeck, K.; Schroeder, F.; Heyden, M.; Fischer, R. A.; Havenith, M. *Phys. Chem. Chem. Phys.* **2008**, *10*, 4732.
(8) Cheng, Y.; Kondo, A.; Noguchi, H.; Kajiro, H.; Urita, K.; Ohba, T.; Kaneko, K.; Kanoh, H. *Langmuir* **2009**, *25*, 4510.
(9) Huang, L. M.; Wang, H. T.; Chen, J. X.; Wang, Z. B.; Sun, J. Y.; Zhao, D. Y.; Yan, Y. S. *Microporous Mesoporous Mater.* **2003**, *58*, 105.
(10) Kaye, S. S.; Dailly, A.; Yaghi, O. M.; Long, J. R. *J. Am. Chem. Soc.* **2007**, *129*, 14176.
(11) Gul-E-Noor, F.; Jee, B.; Poeppl, A.; Hartmann, M.; Himsl, D.; Bertmer, M. *Phys. Chem. Chem. Phys.* **2011**, *13*, 7783.
(12) Peterson, G. W.; Wagner, G. W.; Balboa, A.; Mahle, J.; Sewell, T.; Karwacki, C. J. *J. Phys. Chem. C* **2009**, *113*, 13906.
(13) Yang, J.; Grzech, A.; Mulder, F. M.; Dingemans, T. J. *Chem. Commun.* **2011**, *47*, 5244.
(14) Yoo, Y.; Varela-Guerrero, V.; Jeong, H.-K. *Langmuir* **2011**, *27*, 2652.
(15) Bradley, R. H.; Smith, M. W.; Andreu, A.; Falco, M. *Appl. Surf. Sci.* **2011**, *257*, 2912.
(16) Poiré, E.; Klemberg-Sapieha, J. E.; Martinu, L.; Wertheimer, M. R.; Liang, S.; Barton, S. S.; MacDonald, J. A. *J. Appl. Polym. Sci.: Appl. Polym. Symp.* **1994**, *54*, 185.
(17) Biemmi, E.; Darga, A.; Stock, N.; Bein, T. *Microporous Mesoporous Mater.* **2008**, *114*, 380.
(18) Kusgens, P.; Rose, M.; Senkovska, I.; Frode, H.; Henschel, A.; Siegle, S.; Kaskel, S. *Microporous Mesoporous Mater.* **2009**, *120*, 325.
(19) Dolbier, W. R. *Guide to Fluorine NMR for Organic Chemists*; John Wiley & Sons, Inc.: Hoboken, NJ, 2009.
(20) Maricq, M. M.; Waugh, J. S. *J. Chem. Phys.* **1979**, *70*, 3300.
(21) Shard, A. G.; Munro, H. S.; Badyal, J. P. S *Polym. Commun.* **1991**, *32*, 152.
(22) Godfrey, S. P.; Kinmond, E. J.; Badyal, J. P. S; Little, I. R. *Chem. Mater.* **2001**, *13*, 513.
(23) Chowdhury, P.; Bikkina, C.; Meister, D.; Dreisbach, F.; Gumma, S. *Microporous Mesoporous Mater.* **2009**, *117*, 406.
(24) Liu, J.; Culp, J. T.; Natesakhawat, S.; Bockrath, B. C.; Zande, B.; Sankar, S. G.; Garberoglio, G.; Johnson, J. K. *J. Phys. Chem. C* **2007**, *111*, 9305.
(25) Castillo, J. M.; Vlugt, T. J. H.; Calero, S. *J. Phys. Chem. C* **2008**, *112*, 15934.
(26) Yang, Q.; Zhong, C. *J. Phys. Chem. B* **2006**, *110*, 17776.
(27) Wang, S.; Yang, Q.; Zhong, C. *Sep. Purif. Technol.* **2008**, *60*, 30.
(28) Yang, Q.; Xue, C.; Zhong, C.; Chen, J.-F. *AIChE J.* **2007**, *53*, 2832.
(29) Vishnyakov, A.; Ravikovitch, P. I.; Neimark, A. V.; Bülow, M.; Wang, Q. M. *Nano Lett.* **2003**, *3*, 713.
(30) Liu, Y.; Brown, C. M.; Neumann, D. A.; Peterson, V. K.; Kepert, C. J. *J. Alloys Compd.* **2007**, *446*, 385.
(31) Jorgensen, W. L.; Maxwell, D. S.; TiradoRives, J. *J. Am. Chem. Soc.* **1996**, *118*, 11225.
(32) Rappe, A. K.; Casewit, C. J.; Colwell, K. S.; Goddard, W. A.; Skiff, W. M. *J. Am. Chem. Soc.* **1992**, *114*, 10024.
(33) Watkins, E. K.; Jorgensen, W. L. *J. Phys. Chem. A* **2001**, *105*, 4118.
(34) Petit, C.; Huang, L.; Jagiello, J.; Kenvin, J.; Gubbins, K. E.; Bandosz, T. J. *Langmuir* **2011**, *27*, 13043.